Composites Science and Technology 184 (2019) 107832

Contents lists available at ScienceDirect

Composites Science and Technology

journal homepage: http://www.elsevier.com/locate/compscitech

Manufacturing of unidirectional glass-fiber-reinforced composites via frontal polymerization: A numerical study

S. Vyas [a,c], E. Goli [b,c], X. Zhang [a,c,1], P.H. Geubelle [a,c,*]

[a] Department of Aerospace Engineering, University of Illinois, Urbana, IL, 61801, United States
[b] Department of Civil and Environmental Engineering, University of Illinois, Urbana, IL, 61801, United States
[c] Beckman Institute for Advanced Science and Technology, University of Illinois, Urbana, IL, 61801, United States

ARTICLE INFO

Keywords:
Frontal polymerization
Glass-fiber-reinforced composites
Carbon-fiber-reinforced composites
Thermo-chemical model
Finite element analysis
Dicyclopentadiene

ABSTRACT

Frontal polymerization (FP) is explored as a faster and energy-efficient manufacturing method for dicyclopentadiene (DCPD) matrix, E-glass-fiber-reinforced composites through a series of numerical simulations based on a homogenized reaction-diffusion model. The simulations are carried out over a range of values of fiber volume fraction using (i) a transient, nonlinear, multi-physics finite element solver, and (ii) a semi-analytic steady-state solver. We observe that the front velocity and temperature decrease with an increase in the fiber volume fraction until a critical point is reached, beyond which FP is no longer observed as the front is quenched. To highlight the effect of the material properties of the reinforcing phase, the dependencies of the front velocity, width and maximum temperature on the fiber volume fraction obtained for glass/DCPD composites are compared to those associated with carbon/DCPD composites.

1. Introduction

Due to their high specific strength and stiffness, flexibility and resistance to chemical harm, glass-fiber-reinforced polymer composites (GFRPCs) are found in many structural applications in the aerospace, marine, wind energy, and automotive industries [1]. However, traditional manufacturing processes of composite materials based on autoclaves and heated molds require significant capital investments and have high energy requirements associated with the complex and time-consuming cure cycles involved in the bulk curing of the thermosetting resin [2]. A recently introduced alternative to conventional manufacturing techniques, frontal polymerization (FP), which involves a highly localized and self-propagating exothermic reaction zone converting a monomer into a polymer [3–7], offers a cheaper, faster, and energy-efficient option for manufacturing composites [8].

Multiple mathematical models have been introduced to describe frontal polymerization in a variety of chemicals. Goldfeder et al. [9] and Solovyov et al. [10] used a free-radical polymerization model to solve for the degree of conversion of the monomer to polymer coupled with the heat diffusion equation to describe the process of FP in butyl acrylate and methacrylic acid, respectively. Instead of solving for the conversion of the monomer, phenomenological models based on a cure kinetics relation can be used to simplify the mathematical model [11]. In this line of work, Frulloni et al. [12] developed a finite difference model to describe FP in an epoxy system. Recently, Robertson et al. [8] and Goli et al. [13] used the finite element method to solve the transient, coupled diffusion-reaction equations based on the Prout-Tompkins model [14] to describe FP in DCPD.

In this study, we use the reaction-diffusion relations described in Ref. [8] and homogenize this model to incorporate the effects of the glass fibers on the frontal polymerization of glass/DCPD composites. Using an open-source transient finite element solver, we conduct a detailed parametric study using 1-D simulations to study the effects of the glass fibers on the velocity, width and maximum temperature of the reaction front. We also develop a semi-analytic steady-state formulation, which converts the coupled reaction-diffusion partial differential equations to a system of ordinary differential equations [13], compare the steady-state results to those obtained with the transient finite element solver and use the steady-state solver to quantify the dependence of the front speed on the heat of the reaction.

The present study on glass/DCPD composites builds on the recent work of Robertson et al. [8] and Goli et al. [15], who investigated both experimentally and numerically the feasibility of FP-based manufacturing of carbon/DCPD composites. To demonstrate the

* Corresponding author. Department of Aerospace Engineering, University of Illinois, Urbana, IL, 61801, United States.
E-mail address: geubelle@illinois.edu (P.H. Geubelle).
[1] Current address: Department of Mechanical Engineering, University of Wyoming, Laramie, WY, 82071, United States.

https://doi.org/10.1016/j.compscitech.2019.107832
Received 5 August 2019; Received in revised form 13 September 2019; Accepted 19 September 2019
Available online 25 September 2019

importance of the thermal conductivity of the reinforcing phase alluded to recently in Ref. [16], we also compare the glass/DCPD results to the carbon/DCPD predictions obtained by Goli et al. [15].

The manuscript is organized as follows: The transient and steady-state formulations of the homogenized reaction-diffusion thermo-chemical model used to describe the propagation of a polymerization front in a unidirectional composite are summarized in Sections 2 and 3, respectively. Results from these two models for glass/DCPD composites are presented in Section 4, with emphasis on the effect of the fiber volume fraction on the speed, temperature and intrinsic length scales of the polymerization front. Section 5 compares the characteristics of the polymerization front in glass/DCPD and carbon/DCPD composites.

2. Transient reaction-diffusion model

In the present study, the cure kinetics of FP in DCPD is described using the Prout-Tompkins autocatalytic model with diffusion effects [13]. To simulate the presence of glass fibers in the unidirectional E-glass-fiber-reinforced DCPD composite, we modify the thermal diffusion model by homogenizing the thermal properties of the material. Assuming adiabatic conditions, i.e., in the absence of heat losses to the surrounding, the homogenized reaction-diffusion equations in terms of the temperature T (in K) and degree of cure α (non-dimensional) take the following 1-D form:

$$\begin{cases} \bar{\kappa}\dfrac{\partial^2 T}{\partial x^2} + (1-\varphi)\bar{\rho}H_r\dfrac{\partial \alpha}{\partial t} = \overline{\rho C_p}\dfrac{\partial T}{\partial t}, \\ \dfrac{\partial \alpha}{\partial t} = A exp\left(-\dfrac{E}{RT}\right)(1-\alpha)^n \alpha^m \left(\dfrac{1}{1+exp(c_d(\alpha-\alpha_d))}\right), \end{cases} \tag{1}$$

where x (in m) is the spatial coordinate, t (in s) is time, κ (in $W/(m{\cdot}K)$), ρ (in kg/m^3), and C_p (in $J/(kg{\cdot}K)$) respectively denote the thermal conductivity, density, and heat capacity, H_r (in J/kg) is the enthalpy of reaction, A (in $1/s$) is the pre-exponential time constant, E (in J/mol) is the activation energy, R ($8.314\ J/(mol{\cdot}K)$) is the universal gas constant, φ is the fiber volume fraction, n and m are the two exponents entering the Prout-Tompkins model, while c_d and α_d are two non-dimensional constants introduced to incorporate diffusion effects. The cure kinetics parameters are extracted using Differential Scanning Calorimetry (DSC) experiments on resin samples and applying a nonlinear fitting scheme [14].

The homogenized material properties in the direction of the front propagation are denoted by the overbar and defined as

$$\begin{aligned} \bar{\kappa} &= \kappa_m(1-\varphi) + \kappa_f\varphi, \\ \bar{\rho} &= \rho_m(1-\varphi) + \rho_f\varphi, \\ \overline{C_p} &= C_{pm}(1-\varphi) + C_{pf}\varphi, \end{aligned} \tag{2}$$

where subscripts m and f respectively denote the matrix and the fiber. In this adiabatic setting, the predicted values will be the upper bounds of the front speed and temperature.

The coupled, partial differential reaction-diffusion equations (Eq. (1)) are solved using the open-source, C++, multi-physics finite element solver MOOSE [17]. The solver supports mesh adaptivity, which is pivotal to capture the sharp moving fronts that characterize the cure and temperature solutions. To study the effects of the reinforcing phase on the front velocity, width and temperature, 1-D simulations with values of φ ranging from 0 (pure DCPD) to 0.6 are carried out. In all simulations, the domain is 5 cm long, thermally insulated at both ends, except for $0 \le t \le 1$ s, where a thermal trigger of $210^{\circ}C$ is applied at the left end to initiate the FP reaction.

Assuming that all the heat released during polymerization is used to propagate the front, we define the maximum temperature T_{max} associated with the front as

$$T_{max} = T^0 + (1-\varphi)(1-\alpha_0)\frac{H_r}{\overline{C_p}}, \tag{3}$$

where T^0 (set at $20^{\circ}C$ in this work) is the initial temperature of the resin, and α_0 (set at 0.01) is the initial degree of cure of DCPD. The temperature solution is normalized as follows:

$$\theta = \frac{T - T^0}{T^0_{max} - T^0}, \tag{4}$$

where T^0_{max} refers to the maximum temperature corresponding to $\alpha_0 = 0$, $\overline{C_p} = C_{pm}$, and $\varphi = 0$.

The polymerization fronts are also characterized by two length scales, one (L_θ) for the temperature solution, and the other (L_α) for the degree-of-cure solution. The fronts are very sharp, almost akin to a shock wave in granular media [18]. Based on this similarity, we define the width of the fronts as

$$\begin{cases} L_\theta = \dfrac{\theta_{max}}{\left|\left(\dfrac{\partial \theta}{\partial x}\right)_{max}\right|}, \\ L_\alpha = \dfrac{\alpha_{max}}{\left|\left(\dfrac{\partial \alpha}{\partial x}\right)_{max}\right|}. \end{cases} \tag{5}$$

3. Steady-state formulation

To capture the steady-state propagation of the reaction front, we convert the coupled, partial differential equations to a system of coupled, ordinary differential equations (ODEs) by rewriting the temperature and degree of cure solution in a coordinate frame moving with a steadily propagating polymerization front [13]. This method serves as a more efficient alternative to study the impact of the reinforcing phase and of the cure kinetics on the key characteristics (speed, width and maximum temperature) of the front.

Using Eq. (4) for the non-dimensional form of the temperature T, we adopt the following non-dimensional form of t and x:

$$\tau = At, \bar{x} = \frac{x}{L}, \tag{6}$$

where the length scale L will be determined by the steady-state solver. Substituting Eq. (6) in Eq. (1) yields

$$\begin{cases} \dfrac{\partial \theta}{\partial \tau} = \eta\dfrac{\partial^2 \theta}{\partial \bar{x}^2} + \gamma\dfrac{\partial \alpha}{\partial \tau}, \\ \dfrac{\partial \alpha}{\partial \tau} = f(\theta)g(\alpha), \end{cases} \tag{7}$$

where the non-dimensional coefficients η and γ are defined as

$$\eta = \frac{\bar{\kappa}}{\overline{\rho C_p} AL^2}, \gamma = \frac{(1-\varphi)H_r}{\overline{C_p}\left(T^0_{max} - T^0\right)}. \tag{8}$$

Defining the non-dimensional (constant) front velocity by $W = V_f/AL$, we introduce the coordinate $y = \bar{x} - W\tau$ associated with the front and rewrite Eq. (7) as the following system of ODEs:

$$\begin{cases} \dfrac{d^2\widehat{\theta}}{dy^2} + W\dfrac{d\widehat{\theta}}{dy} - \gamma W\dfrac{d\widehat{\alpha}}{dy} = 0, \\ W\dfrac{d\widehat{\alpha}}{dy} + f(\widehat{\theta})g(\widehat{\alpha}) = 0. \end{cases} \tag{9}$$

The steady-state problem is solved by combining an explicit finite difference scheme to integrate the ODEs over the interval $0 \le y \le 1$, and an iterative scheme to determine the two unknowns, L and V_f, which

Table 1
Thermal conductivity, density, specific heat capacity, and thermal diffusivity of DCPD, E-glass-fibers and carbon fibers [19].

	$\kappa\left(\frac{W}{m.K}\right)$	$\rho\left(\frac{kg}{m^3}\right)$	$C_p\ \left(\frac{J}{kg.K}\right)$	$\lambda\left(\frac{m^2}{s}\right)$
DCPD	0.15	980.0	1600.0	$9.69*10^{-8}$
E-glass fibers	1.28	2575.0	802.5	$6.17*10^{-7}$
Carbon fibers	9.38	1800.0	753.6	$6.90*10^{-6}$

Table 2
Cure kinetics parameters of the PT model (Eq. (1)) for DCPD.

$A\left(\frac{1}{s}\right)$	$E\left(\frac{J}{mol}\right)$	$H_r\left(\frac{J}{g}\right)$	n	m	c_d	α_d
$8.55*10^{15}$	110750.0	350.0	1.72	0.77	14.48	0.41

satisfy boundary conditions

$$\begin{cases} \widehat{\theta}(y=0)=\theta_{max}, \quad \widehat{\theta}(y=1)=0, \\ \dfrac{d\widehat{\theta}}{dy}(y=0)=0, \quad \dfrac{d\widehat{\theta}}{dy}(y=1)=0, \\ \widehat{\alpha}(y=0)=1-\varepsilon, \quad \widehat{\alpha}(y=1)=\alpha_0, \end{cases} \tag{10}$$

where θ_{max} refers to the maximum non-dimensional temperature corresponding to T_{max} and $\varepsilon \ll 1$.

4. Results

The resin of interest in this study is DCPD mixed with Grubb's 2nd-generation catalyst and 0.5 molar equivalent of tri-butyl phosphite, an inhibitor introduced to increase the pot life of the monomer [8]. The material properties (including the diffusivity λ) considered in this study are presented in Table 1, while the cure kinetics parameters for the DCPD resin are presented in Table 2.

In all finite element simulations, the solution for the temperature and degree of cure goes first through a transient phase associated with the initial triggering of the polymerization front, before transitioning to a steady-state regime with a constant front velocity that depends on the fiber volume fraction. Fig. 1 shows the normalized temperature and degree of cure solutions after steady-state conditions have been reached, for three values of the fiber volume fraction: $\varphi = 0$, 0.2 and 0.4. As apparent in that figure, the maximum temperature behind the front decreases with increasing value of φ due to the reduction in available energy of reaction as the relative portion of resin decreases with increasing fiber volume fraction, as captured by the $(1-\varphi)$ coefficient present in the exothermic source term in the thermal equation (1). As also apparent in Fig. 1, the sharpness of the front decreases with increasing fiber volume fraction due to the higher thermal conductivity of the glass fibers.

Fig. 2 summarizes the results of the parametric finite element study by presenting the dependence of the front velocity V_f (left axis) and maximum temperature T_{max} (right axis) on the fiber volume fraction φ. Also included in the figure is the analytical (diffusion-free) prediction (shown as a dotted curve) of the maximum temperature described by Eq. (3).

The dependence of V_f on φ illustrates the competition between two key mechanisms. As the fiber volume fraction increases, the energy available for the frontal polymerization decreases due to the aforementioned $(1-\varphi)$ coefficient present in the exothermic source term in Eq. (1). At the same time, the effective thermal conductivity $\bar{\kappa}$ of the composite increases with increasing values of φ, which tends to speed up

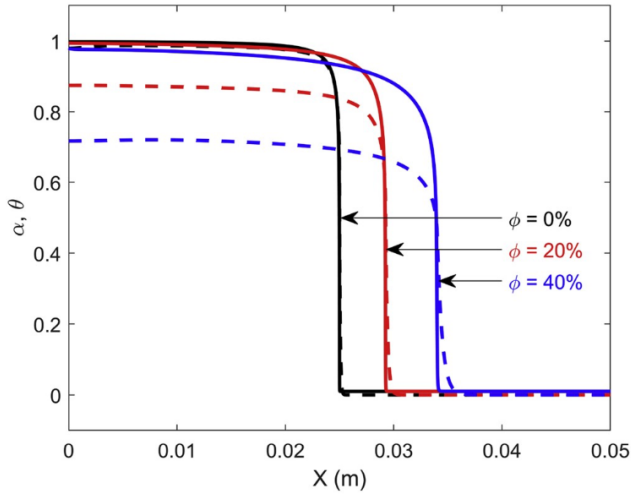

Fig. 1. Finite element prediction of the degree of cure (solid curves) and temperature (dashed curves) profiles in the steady-state regime for $\varphi = 0$, 0.2, and 0.4, showing the reduction in front temperature and sharpness with increasing fiber volume fraction.

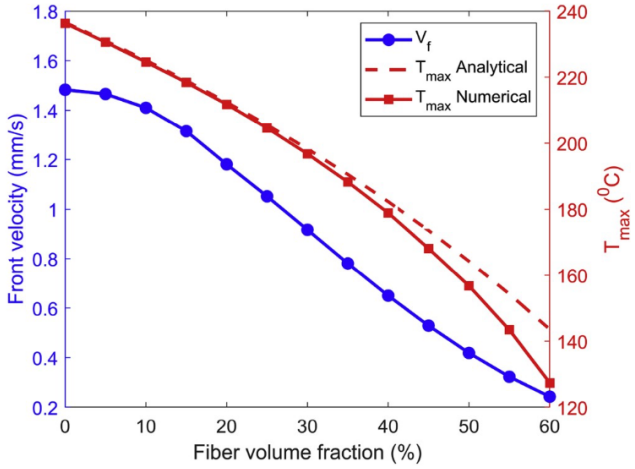

Fig. 2. Dependence of the front velocity and temperature on the fiber volume fraction. The growing difference between the analytical prediction Eq. (3) and the numerical solution for the front temperature for higher values of φ shows the increasing effect of thermal diffusion due to the reinforcing phase.

the polymerization front. This latter mechanism is expected to play a bigger role for small values of the fiber volume fraction. Due to the relatively small thermal conductivity of E-glass fibers compared to that of carbon fibers (See Section 5), this effect is marginal and limited to very small values of the fiber volume fraction ($\varphi < 0.05$), and the reduction of heat of reaction with increase in fiber volume fraction leads to a monotonic reduction in the speed of the polymerization front for $\varphi > 0.05$.

The front temperature also decreases monotonically with the fiber volume fraction. As apparent in Fig. 2, the analytical, diffusion-free prediction given by Eq. (3) captures this dependence very well for $0 \leq \varphi \leq 0.4$. For higher values of the fiber volume fraction, the increase in diffusivity, which led to the smoothing of the front observed in Fig. 1, yields a separation between numerical and analytical predictions of T_{max}, with the diffusion-free prediction serving as an upper bound.

Fig. 3 shows the effect of the fiber volume fraction on the two length scales L_α and L_θ that define the width of the front and were introduced earlier in Eq. (5). As apparent in Fig. 3 and alluded to in Fig. 1, the

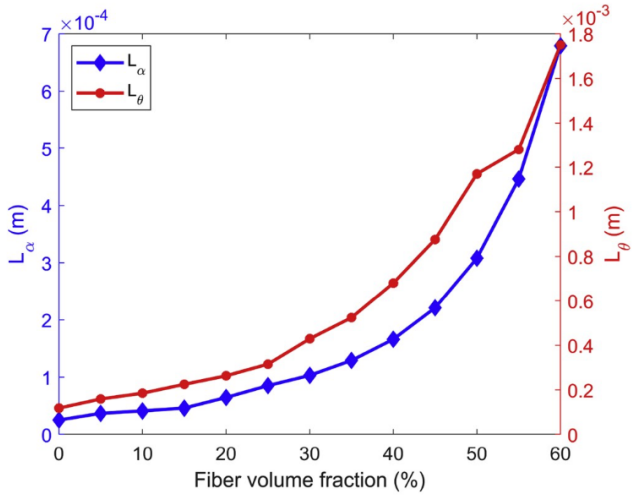

Fig. 3. Evolution of the intrinsic length scales L_α and L_θ of the front defined by Eq. (5) on the fiber volume fraction, showing the smoothing of the front as φ increases, as was alluded to in Fig. 1.

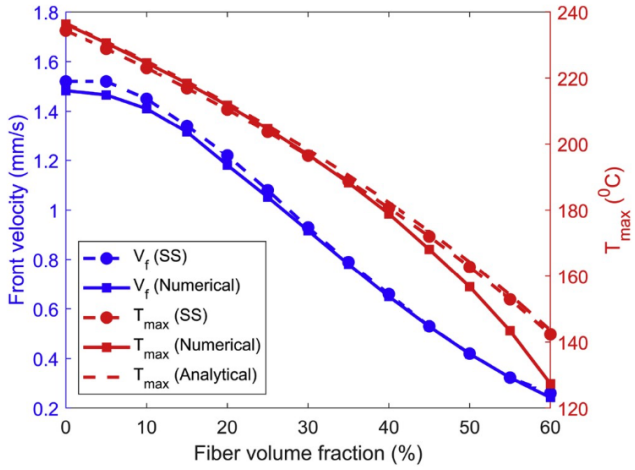

Fig. 4. Comparison between transient (Numerical) and steady-state (SS) predictions of the φ-dependence of the front velocity and maximum temperature. The analytical 'diffusion-free' prediction Eq (3) of the maximum temperature is also shown.

addition of fibers reduces the sharpness of the front due to the increasing role of the thermal diffusivity. The results also show the temperature tends to rise over a distance between 2 and 2.5 times wider than the degree of cure.

Fig. 4 presents the dependence of the frontal velocity and maximum temperature on the fiber volume fraction obtained from the steady-state model and compares the results to those extracted from the transient solution. While the velocity results are in good agreement for all values of φ, we observe some differences between the maximum temperature values provided by the transient finite element solver and the steady-state formulation. This difference can be explained by the fact that the steady-state formulation uses the analytical prediction for the maximum temperature in the definition of the boundary conditions at $y = 0$. It is therefore natural that the steady-state and analytical expressions of T_{max} agree. Furthermore, the analytical prediction assumes that the monomer has fully polymerized as expressed by the $(1-\alpha_0)$ factor in Eq. (3). However, as apparent in Fig. 1, the degree of cure computed with the transient solver at the left end of the 5 cm domain decreases as the concentration of the fiber volume fraction increases. This decrease in the

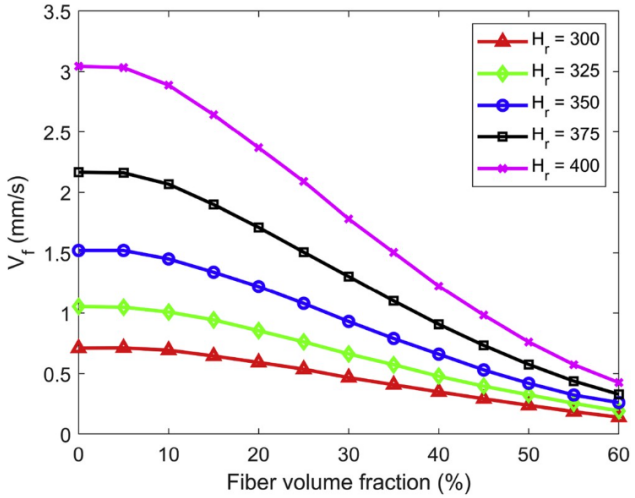

Fig. 5. Effect of the total heat of the reaction H_r (given in J/g) on the front velocity for glass/DCPD composites. The curve corresponding to $H_r = 350\ J/g$ is the reference curve shown in Fig. 2.

maximum value of the degree of cure leads to a similar reduction in the maximum temperature obtained by the transient finite element solver, and this effect is especially prominent for higher values of φ. A substantially larger domain and longer simulation time would be needed to further increase the maximum value of α to 1 and achieve a closer agreement between the numerical, steady-state, and analytical values of T_{max}.

Taking advantage of the efficiency of the steady-state solver, we can perform a parametric study of the impact of cure kinetics parameters on the characteristics of the front. An example of such a study is shown in Fig. 5, which presents how the heat of reaction, H_r, impacts the front velocity in glass/DCPD composites with $0 \leq \varphi \leq 0.6$. As expected, a higher value of H_r leads to a faster front and might extend the range of applicability of FP to higher fiber volume fraction values. For reference, the 65 data-points shown in Fig. 5 were obtained in approximately 12.5 min with the steady-state formulation, while a single finite element simulation typically takes a couple of hours due to the high level of spatial and temporal adaptivity involved.

5. Comparison between glass/DCPD and carbon/DCPD composites

In a recent study, Goli et al. [15] have shown that FP is a viable manufacturing method for unidirectional carbon-fiber-reinforced DCPD-matrix composites. The authors implemented a similar reaction-diffusion model to perform simulations of the initiation and propagation of the front in carbon/DCPD composites, and validated the model against experimental measurements of the front speed and temperature obtained for various values of the fiber volume fraction.

In this section, we present a comparison between the results of FP simulations in glass-DCPD and carbon-DCPD to assess the impact of the reinforcing phase on the speed, width and temperature of the front. The thermal properties of the carbon fibers used in the study were provided in Table 1, while the cure kinetics model for DCPD and boundary conditions adopted in the carbon/DCPD simulations are the same as those used for the glass/DCPD composite system described in the previous section. As was the case for the glass/DCPD composites, FP is initiated by applying a thermal trigger of $210°C$ for $1\ s$ at the left edge of the domain, with insulated boundary conditions at both ends adopted for the remainder of the simulation.

As indicated earlier (Fig. 2), the φ-dependence of the front velocity in the glass/DCPD composites is monotonically decreasing, except,

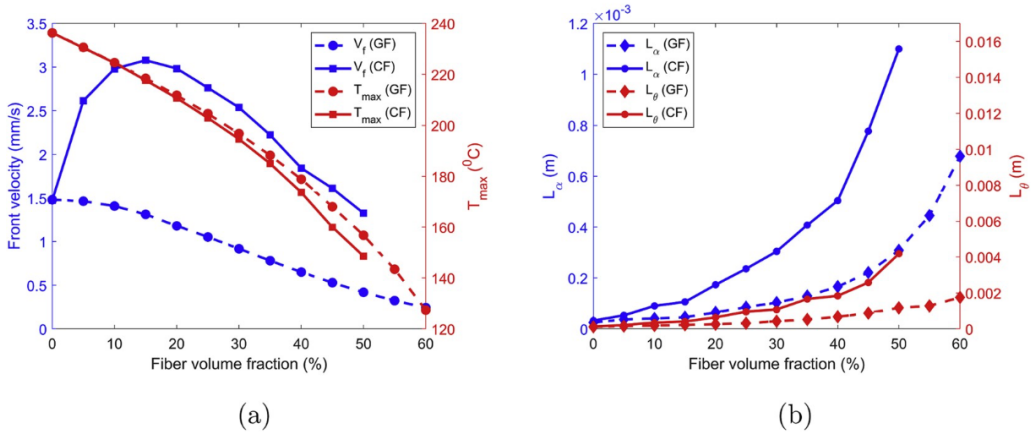

Fig. 6. Comparison between the FP of glass/DCPD (GF) and carbon/DCPD (CF) composites: φ-dependence of the front velocity and maximum temperature (a) and of the characteristic lengths (b). The difference observed in the φ-dependence of V_f, L_α, L_θ, and quenching limit can be attributed to the sharp contrast in thermal diffusivity between the reinforcing phases.

marginally, for very small values of the fiber volume fraction. As illustrated in Fig. 6a, the solution is quite different for carbon/DCPD composites, where the higher thermal conductivity of the carbon fibers leads to a substantial increase in V_f, with a maximum in excess of 3 mm/s corresponding to $\varphi = 0.2$ before a progressive reduction of the front speed as φ further increases. The φ-dependence of the front temperature is relatively similar for both composites, with the higher effective conductivity of the carbon/DCPD composites yielding a slightly lower front temperature than its glass/DCPD counterpart. It should also be noted that the higher thermal diffusivity of the carbon fibers leads to a lower quenching limit defined as the highest fiber volume fraction for which the front can be initiated based on the applied 1 s thermal trigger. While the maximum fiber volume fraction achievable for a FP-manufactured glass/DCPD composite is about 0.6, it is reduced to about 0.5 for the carbon/DCPD composite. To achieve higher fiber volume fractions, a different cure kinetics and/or thermal trigger would be needed.

Fig. 6b presents the effect of the reinforcing phase on L_α and L_θ, showing a much sharper polymerization front in glass/DCPD than in carbon/DCPD, especially at higher values of the fiber volume fraction.

6. Conclusion

In this paper, we have explored numerically the feasibility of frontal polymerization as a manufacturing process for E-glass-fiber-reinforced composites. The frontal polymerization process has been described by a system of coupled thermo-chemical equations, with the effects of the reinforcing phase captured through homogenized thermal properties and through a reduction in the available heat of reaction. The effects of the fiber volume fraction on the velocity, width and maximum temperature of the polymerization front have been studied using an adaptive finite-element transient solver and a semi-analytic steady-state solver.

The model has been shown to capture the two competing effects of the fiber volume fraction. On one hand, the increase in thermal diffusivity associated with the homogenized model leads to a positive effect of the fiber content on the front speed and on the smoothing of the front. On the other hand, the heat released by the exothermic polymerization decreases with increasing fiber volume fraction, thereby reducing the front velocity. These competing effects lead to a non-monotonic dependence of the front speed on the fiber volume fraction. This effect is especially visible for the carbon/DCPD composites due to the high mismatch in thermal diffusivity between the fibers and the resin. Due to the relatively lower thermal diffusivity of the E-glass fibers, the second effect dominates, leading to a monotonically decreasing trend of the front speed with respect to the fiber volume fraction.

Acknowledgement

This work was supported by the Air Force Office of Scientific Research through Award FA9550-16-1-0017 (Dr. B. 'Les' Lee, Program Manager) as part of the Center for Excellence in Self-Healing, Regeneration, and Structural Remodeling. This work was also supported by the National Science Foundation (NSF Grant No. 1830635), through the LEAP HI: Manufacturing USA program. The authors would like to acknowledge Prof. Scott White for his insights and guidance regarding this work.

References

[1] T. Sathishkumar, S. Satheeshkumar, J. Naveen, Glass fiber-reinforced polymer composites–a review, J. Reinf. Plast. Compos. 33 (13) (2014) 1258–1275.
[2] D. Abliz, Y. Duan, L. Steuernagel, L. Xie, D. Li, G. Ziegmann, Curing methods for advanced polymer composites-a review, Polym. Polym. Compos. 21 (6) (2013) 341–348.
[3] J. Pojman, V. Ilyashenko, A. Khan, Free-radical frontal polymerization: self-propagating thermal reaction waves, J. Chem. Soc., Faraday Trans. 92 (16) (1996) 2825–2837.
[4] J. Pojman, G. Curtis, V. Ilyashenko, Frontal polymerization in solution, J. Am. Chem. Soc. 118 (15) (1996) 3783–3784.
[5] D. Fortenberry, J. Pojman, Solvent-free synthesis of polyacrylamide by frontal polymerization, J. Polym. Sci. A Polym. Chem. 38 (7) (2000) 1129–1135.
[6] A. Mariani, S. Fiori, Y. Chekanov, J. Pojman, Frontal ring-opening metathesis polymerization of dicyclopentadiene, Macromolecules 34 (19) (2001) 6539–6541.
[7] S. Davtyan, A. Berlin, A. Tonoyan, Advances and problems of frontal polymerization processes, Rev. J. Chem. 1 (1) (2011) 56–92.
[8] I. Robertson, M. Yourdkhani, P. Centellas, J. Aw, D. Ivanoff, E. Goli, E. Lloyd, L. Dean, N. Sottos, P. Geubelle, J. Moore, S. White, Rapid energy-efficient manufacturing of polymers and composites via frontal polymerization, Nature 557 (7704) (2018) 223.
[9] P. Goldfeder, V. Volpert, V. Ilyashenko, A. Khan, J. Pojman, S. Solovyov, Mathematical modeling of free-radical polymerization fronts, J. Phys. Chem. B 101 (18) (1997) 3474–3482.
[10] S. Solovyov, V. Ilyashenko, J. Pojman, Numerical modeling of self-propagating polymerization fronts: the role of kinetics on front stability, Chaos: Interdiscip. J. Nonlinear Sci. 7 (2) (1997) 331–340.
[11] E. Turi, Thermal Characterization of Polymeric Materials, Elsevier, 2012.
[12] E. Frulloni, M. Salinas, L. Torre, A. Mariani, J. Kenny, Numerical modeling and experimental study of the frontal polymerization of the diglycidyl ether of bisphenol a/diethylenetriamine epoxy system, J. Appl. Polym. Sci. 96 (5) (2005) 1756–1766.
[13] E. Goli, I. Robertson, P. Geubelle, J. Moore, Frontal polymerization of dicyclopentadiene: a numerical study, J. Phys. Chem. B 122 (16) (2018) 4583–4591.
[14] M. Kessler, S. White, Cure kinetics of the ring-opening metathesis polymerization of dicyclopentadiene, J. Polym. Sci. A Polym. Chem. 40 (14) (2002) 2373–2383.
[15] E. Goli, N. Parikh, M. Yourdkhani, N. Hibbard, J. Moore, N. Sottos, P. Geubelle, Frontal Polymerization of Unidirectional Carbon-Fiber-Reinforced Composites, (submitted for publication).
[16] E. Goli, I. Robertson, H. Agarwal, E. Pruitt, J. Grolman, P. Geubelle, J. Moore, Frontal polymerization accelerated by continuous conductive elements, J. Appl. Polym. Sci. 136 (17) (2019) 47418.

[17] D. Gaston, C. Newman, G. Hansen, D. Lebrun-Grandie, Moose: a parallel computational framework for coupled systems of nonlinear equations, Nucl. Eng. Des. 239 (10) (2009) 1768–1778.

[18] L. Gómez, A. Turner, V. Vitelli, Uniform shock waves in disordered granular matter, Phys. Rev. E 86 (4) (2012), 041302.

[19] Properties: E-glass fibre. https://www.azom.com/properties.aspx?ArticleID=764.